

## CHAPTER 4

# Equilibrium Traffic Flow Models

In the previous chapter, it was shown that the following relationship holds among flow  $q$ , density  $k$ , and space mean speed  $\nu$  (the subscript “ $s$ ” is dropped unless it is necessary to distinguish space mean speed  $\nu_s$  from time mean speed  $\nu_t$ ):

$$q = k \times \nu.$$

This relationship is an *identity* since it is self-guaranteed under the generalized definition. One may wish to know what other relationships exist among the three traffic flow characteristics. For example, is there any pairwise relationship between flow and density, density and speed, and speed and density? This chapter attempts to address these questions.

### 4.1 SINGLE-REGIME MODELS

Let us start with field observations. Figure 4.1 illustrates an image captured by a point sensor (a video camera in Georgia NaviGAtor, Georgia’s intelligent transportation system). The point sensor constitutes an observation station consisting of a group of imaginary detectors with one detector in each lane.

As discussed before, traffic data can be extracted from video images by means of image processing. Figure 4.2 shows a portion of a daily report from a video camera. Each row represents observations aggregated over 20 s over all lanes. Column A contains the station ID, column B contains the time stamp of each observation, column C contains the status of the detectors of this station (there are four lanes at this station and hence there are four detectors. “OK” means the corresponding detector is working properly, while “NO\_ACT” means no actuation), columns E through H contain classified traffic counts (only column E is shown here because of limited space), column I contains the occupancy, column K contains the time mean speed, column M contains the average vehicle length, and column P contains the density (estimated by a proprietary recipe).

The point sensor data are plotted in Figure 4.3, where the top-left plot shows the speed-density relationship, the top-right plot shows the speed-flow relationship, the bottom-left plot shows the flow-density



**Figure 4.1** An image captured by a point sensor. (From NaviGAtor.)

relationship, and the bottom-right plot shows the speed-spacing relationship. The “cloud” in Figure 4.3 represents 1 year’s worth of field observations aggregated to 5 min (i.e., each point in the figure represents the traffic condition observed in 5 min). The traffic speed here is the time mean speed since it is impossible to calculate the space mean speed from aggregated point sensor data. Density is estimated from flow and speed. The large dots represent the average of the “cloud.” The plots in Figure 4.3 were generated with use of traffic data collected at a fixed location. Therefore, such plots are location specific—that is, plots generated from different locations may differ. In addition, time information is lost in the figure—that is, one could not deduce the time when a data point was observed. As such, the figure actually depicts an *equilibrium* or *steady-state* relationship. Consequently, models of such a relationship without a reference to time are termed “equilibrium models” or “steady-state models.”

Noticeably, each plot in Figure 4.3 exhibits a trend which suggests a pairwise relationship among flow, speed, and density, though such a relationship is of statistical significance. For example, the top-left plot reveals a decreasing relationship between speed and density with two intercepts intuitively known. The intercept on the space  $x$ -axis represents a “Sunday morning” scenario where there are very few vehicles on the road (i.e.,  $k \rightarrow 0$ ). Hence, one may drive at the desired speed without being blocked by a slow driver ( $v \rightarrow v_f$ , the free-flow speed). The other intercept corresponds to a “Friday afternoon peak” scenario where everyone rushes home. As such, the road is jammed ( $k \rightarrow k_j$ , the jam density), resulting

A	B	C	E	I	K	M	P	Q
#station_id	sample_start	status	volume_auto	time_occupancy	time_speed	length	density	gap
803	4001134 2003-10-08 05:41:00 000 EDT	INO_ACTOKIOKOK	6	0.014	49.1503	14.7638	8.1	796.9
804	4001134 2003-10-08 05:41:20 000 EDT	OKIOKIOKOK	23	0.0276	47.4313	14.5451	13.873	383.8095
805	4001134 2003-10-08 05:41:40 000 EDT	OKIOKIOKOK	17	0.031	48.2745	14.5607	15.5	353.4524
806	4001134 2003-10-08 05:42:00 000 EDT	OKIOKIOKOK	20	0.0473	46.1478	14.7638	18.6429	292.9821
807	4001134 2003-10-08 05:42:20 000 EDT	OKIOKIOKOK_ACT	9	0.0136	53.0384	14.7638	6.7143	761.4286
808	4001134 2003-10-08 05:42:40 000 EDT	OKIOKIOKOK	14	0.02	48.8921	14.7638	11.1579	895.8947
809	4001134 2003-10-08 05:43:00 000 EDT	OKIOKIOKOK	8	0.0086	45.0776	14.7638	5.8782	1055.6882
810	4001134 2003-10-08 05:43:20 000 EDT	OKIOKIOKOK	13	0.0252	50.8922	13.8642	10.7742	538.0645
811	4001134 2003-10-08 05:43:40 000 EDT	OKIOKIOKOK	8	0.0221	52.8492	14.7638	11.2632	619.4211
812	4001134 2003-10-08 05:44:00 000 EDT	OKIOKIOKNO_ACT	10	0.0138	54.9913	14.7638	7.375	779
813	4001134 2003-10-08 05:44:20 000 EDT	OKIOKIOKOK	17	0.019	50.2191	14.7638	10.7	1558.74
814	4001134 2003-10-08 05:44:40 000 EDT	OKIOKIOKOK	14	0.0446	44.9162	14.7638	19.8	295.2571
815	4001134 2003-10-08 05:45:00 000 EDT	OKIOKIOKOK	24	0.0557	43.5066	17.0135	18.2857	295.1857
816	4001134 2003-10-08 05:45:20 000 EDT	OKIOKIOKOK	15	0.0372	49.8987	14.7638	17.6522	439.5217
817	4001134 2003-10-08 05:45:40 000 EDT	OKIOKIOKOK	8	0.0115	50.9524	14.7638	6.7	1667.55
818	4001134 2003-10-08 05:46:00 000 EDT	OKIOKIOKOK	18	0.0229	49.7929	14.7638	11.5556	461.1111
819	4001134 2003-10-08 05:46:20 000 EDT	INO_ACTOKIOKOK	8	0.0236	51.4406	14.7638	10.2143	544.3571
820	4001134 2003-10-08 05:46:40 000 EDT	OKIOKIOKOK	6	0.0092	46.555	14.7638	4.1538	1429.615
821	4001134 2003-10-08 05:47:00 000 EDT	OKIOKIOKOK	14	0.0239	51.5573	14.7638	12.1842	1225.237
822	4001134 2003-10-08 05:47:20 000 EDT	OKIOKIOKOK	24	0.04	45.6946	14.7638	21.2769	330.6923
823	4001134 2003-10-08 05:47:40 000 EDT	OKIOKIOKOK	11	0.0309	44.9755	19.685	11.7812	484.8125
824	4001134 2003-10-08 05:48:00 000 EDT	OKIOKIOKOK	6	0.0094	49.6365	14.7638	4.8824	1318
825	4001134 2003-10-08 05:48:20 000 EDT	OKIOKIOKOK	8	0.0125	49.4766	14.7638	4.875	1271
826	4001134 2003-10-08 05:48:40 000 EDT	OKIOKIOKOK	16	0.0495	47.9935	14.7638	23.0476	253.7381
827	4001134 2003-10-08 05:49:00 000 EDT	OKIOKIOKOK	26	0.0421	47.6679	14.7638	20.1429	578.4935
828	4001134 2003-10-08 05:49:20 000 EDT	OKIOKIOKOK	23	0.0577	49.0984	16.0946	20.3115	265.3279
829	4001134 2003-10-08 05:49:40 000 EDT	OKIOKIOKOK	20	0.0412	47.9673	14.7638	20.451	268.1961
830	4001134 2003-10-08 05:50:00 000 EDT	OKIOKIOKOK	14	0.0334	44.5611	14.3701	13.9714	464.8887
831	4001134 2003-10-08 05:50:20 000 EDT	OKIOKIOKOK	15	0.0303	48.8531	14.7638	13.7027	404.027
832	4001134 2003-10-08 05:50:40 000 EDT	OKIOKIOKOK	25	0.0488	45.2629	14.7638	24.7344	250.25
833	4001134 2003-10-08 05:51:00 000 EDT	OKIOKIOKOK	23	0.0549	44.1544	14.7638	27.6667	199.3881

Figure 4.2 Point sensor data.

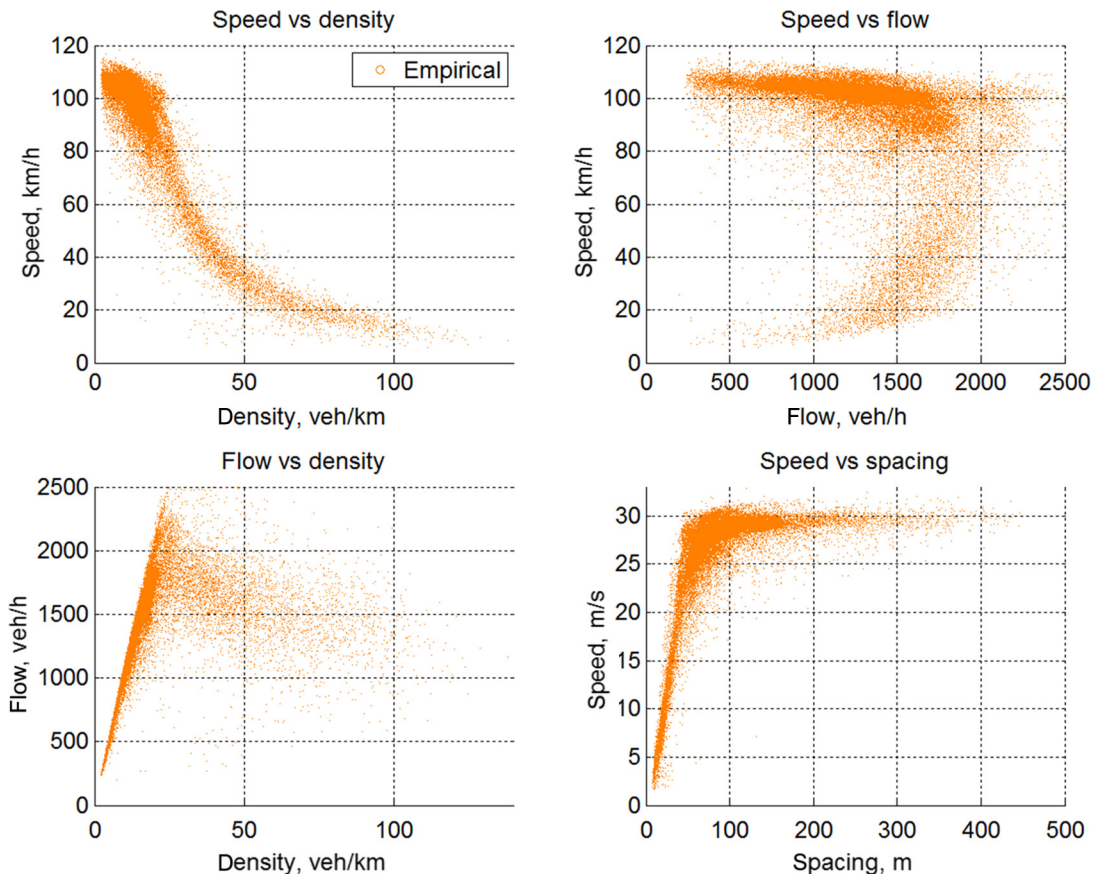


Figure 4.3 Observed  $q$ - $k$ - $v$  relationships.

in a stop-and-go condition ( $v \rightarrow 0$ ). Except for the two intercepts, the remaining trend of the speed-density relationship is debatable, having been debated over the years, and is still debated today. Some examples of historical efforts on this subject are given below.

#### 4.1.1 The Greenshields Model

Since the exact relationship between speed and density is unclear, Greenshields [9] proposed the use of a linear function to summarize the speed-density relationship. Such a function can be completely determined from knowledge of two points on the line: ( $k = 0, v = v_f$ ) and ( $k = k_j, v = 0$ ). Hence, the speed-density  $v$ - $k$  relationship (illustrated in Figure 4.4) can be expressed as

$$v = v_f \left(1 - \frac{k}{k_j}\right).$$

Combining the identity  $q = k \times v$  and eliminating  $v$ , one is able to derive the flow-density  $q$ - $k$  relationship implied by the Greenshields model (Figure 4.5):

$$q = v_f \left(k - \frac{k^2}{k_j}\right).$$

It is interesting to note a few special points on the curve. When the density is close to zero ( $k \rightarrow 0$ ), the flow drops to zero ( $q \rightarrow 0$ ) since the road is almost empty; when the road is jammed ( $k = k_j$ ), the flow also becomes zero ( $q = 0$ ) because no one can move. In addition, since this is

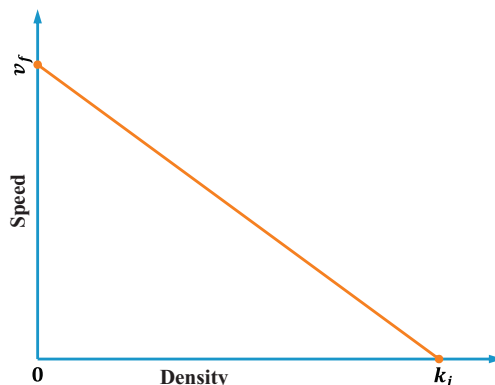


Figure 4.4 The Greenshields speed-density relationship.

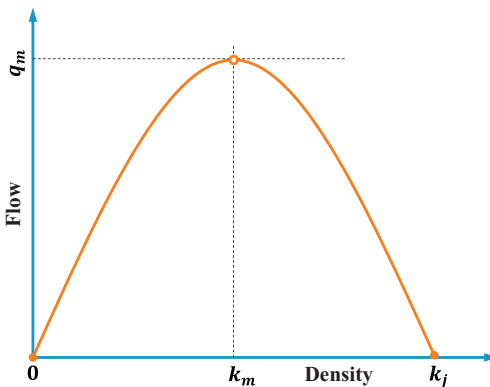


Figure 4.5 Greenshields flow-density relationship.

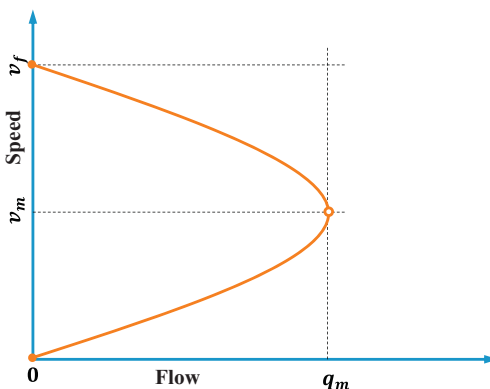


Figure 4.6 Greenshields speed-flow relationship.

a quadratic function with a negative second-order term, the corresponding  $q$ - $k$  curve is parabolic with a downward opening. Therefore, starting from the origin ( $k = 0, q = 0$ ), flow increases as density increases. This trend continues until, at some point ( $k = k_m$ ), the flow peaks ( $q = q_m = \frac{v_f k_j}{4}$ ). After this point, the flow begins to drop as the density continues to increase, and the flow becomes zero ( $q = 0$ ) when the density reaches the jam density ( $k = k_j$ ). In this notation,  $q_m$  is the maximum flow—that is, the capacity—and  $k_m$  is the optimal density—that is, the density when the flow peaks.

Similarly, one can eliminate  $k$  from the Greenshields model by using the identity and obtain a speed-flow  $v$ - $q$  relationship (Figure 4.6):

$$q = k_j \left( v - \frac{v^2}{v_f} \right).$$

This is again a quadratic function with an opening to the left. When the flow is close zero ( $q \rightarrow 0$ ), two scenarios are possible: (1) the road is nearly empty and the few vehicles on the road are able to move at free-flow speed ( $v \rightarrow v_f$ ); (2) the road is jammed, so that no one is able to move ( $v \rightarrow 0$ ). Actually, entering a given flow value less than the capacity into the equation will normally result in two speeds: a lower one, which corresponds to a worse traffic condition, and a higher one, corresponding to a better traffic condition. When the flow reaches capacity ( $q = q_m$ ), the two speeds become one, which is called the optimal speed,  $v_m$ .

Figure 4.7 summarizes the above discussion graphically and puts the speed-density, flow-density, and speed-flow relationships together. Remark-

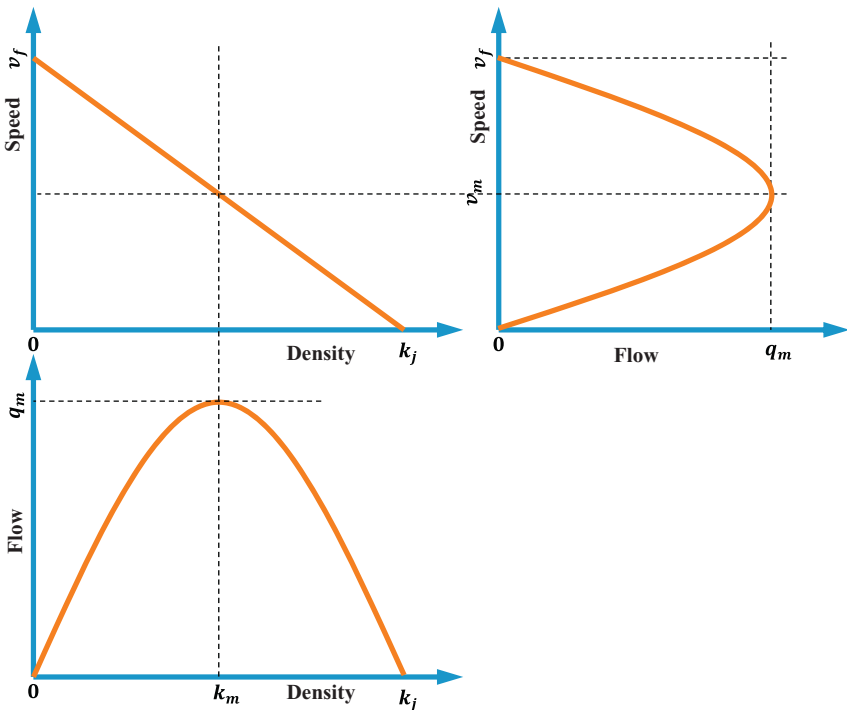


Figure 4.7 Greenshields flow-density-speed relationship.

ably, the relationships among flow, speed, and density such as those depicted in [Figure 4.3](#) and modeled in [Figure 4.7](#) are unique to vehicular traffic flow and are not observed in any other kind of flow, such as gas flow, fluid flow, and flow of Internet packets. Hence, the model and its associated graphical representation that summarizes the pairwise relationships among traffic flow characteristics are the distinguishing features of vehicular traffic flow. Therefore, they are referred to as the *fundamental diagram* in traffic flow theory. The work by Greenshields depicted in [Figure 4.7](#) constitutes the first fundamental diagram in traffic flow theory.

Note that the three pairwise relationships—that is, the speed-density, flow-density, and speed-flow relationships—reflect different facets of the flow-speed-density relationship. Hence, they have different applications in traffic flow theory. For example, the speed-density relationship relates a driver's speed choice to the concentration of vehicles around the driver. Therefore, the relationship is typically used in traffic flow theory to understand how drivers adjust their speeds in response to traffic in their vicinity—that is, modeling drivers' car-following behavior. As will be seen later, the flow-density relationship is convenient for explaining the propagation of disturbances in traffic flow (such as waves and their velocities) and, hence, is frequently used in dynamic traffic flow modeling. Anyone who is familiar with highway capacity and level of service (LOS) will immediately recognize that the speed-flow relationship is extensively used by traffic engineers to perform highway capacity analysis and determine the LOS on freeways and multilane highways.

### 4.1.2 Other Single-Regime Models

Owing to its simplicity and elegance, the Greenshields model, together with its associated fundamental diagram, is ideal for illustration and pedagogical purposes. Empirical observations reveal that the model suffers from a lack of accuracy, which is salient in [Figure 4.8](#), where the Greenshields model is plotted on top of field observations. For example, the model predicts that the capacity ( $q = q_m$ ) occurs at half the jam density ( $k_m = \frac{1}{2}k_j$ ). If an average vehicle length of 6 m or 20 feet is assumed, the jam density would be somewhere around  $1000/6 \approx 164$  vehicles per kilometer or  $5280/20 \approx 264$  vehicles per mile. Half of this number is 82 vehicles per kilometer or 132 vehicles per mile. However, field observations suggest that  $k_m$  is most likely in the range of 25–40 vehicles per kilometer or 40–65 vehicles per mile. In addition, unlike the way that speed decreases linearly with density, field observations show that free-flow speed can be sustained up to a density

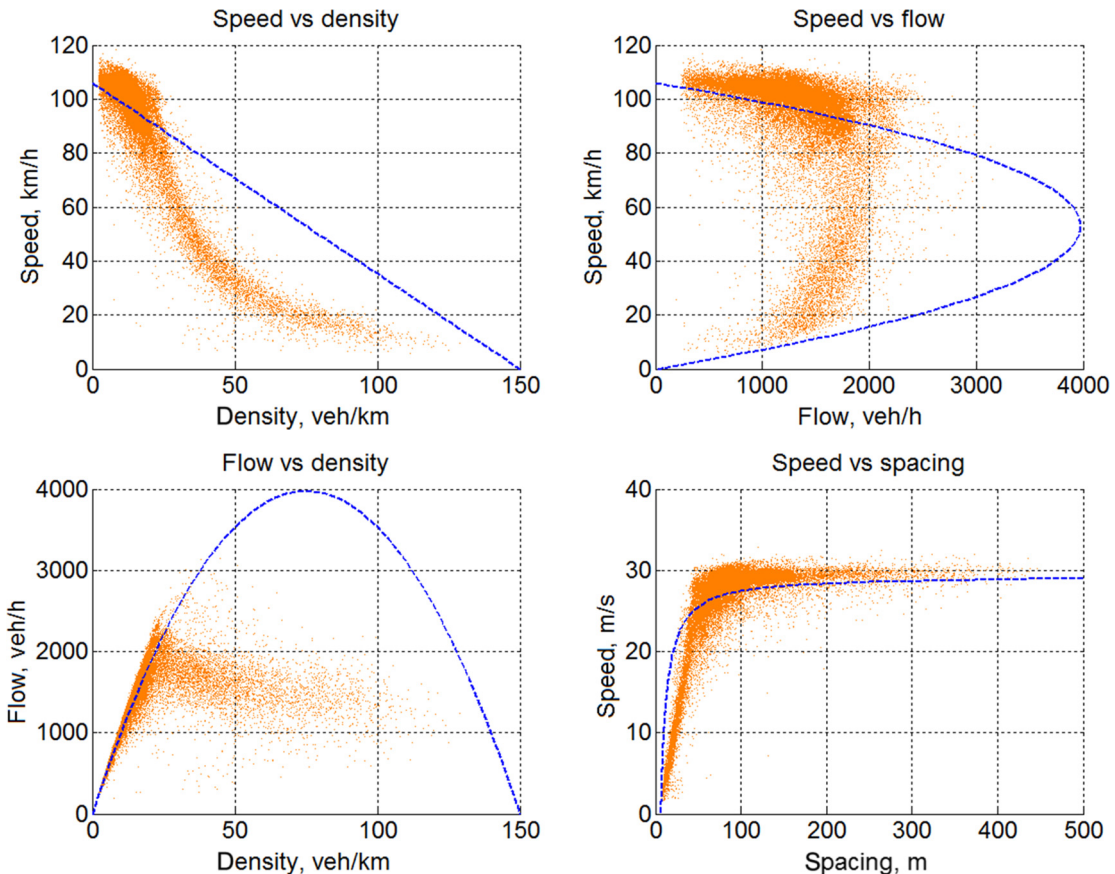


Figure 4.8 Fundamental diagrams implied by Greenshields model.

**Table 4.1** Single-regime models

Authors	Model	Parameters
Greenshields [9]	$v = v_f \left(1 - \frac{k}{k_j}\right)$	$v_f, k_j$
Greenberg [10]	$v = v_m \ln \left(\frac{k_j}{k}\right)$	$v_m, k_j$
Underwood [11]	$v = v_f e^{-\frac{k}{k_m}}$	$v_f, k_m$
Drake et al. [12]	$v = v_f e^{-\frac{1}{2} \left(\frac{k}{k_m}\right)^2}$	$v_f, k_m$
Drew [13]	$v = v_f \left[1 - \left(\frac{k}{k_j}\right)^{n+\frac{1}{2}}\right]$	$v_f, k_j, n$
Pipes [14] and Munjal [15]	$v = v_f \left[1 - \left(\frac{k}{k_j}\right)^n\right]$	$v_f, k_j, n$

$v_f$  is free-flow speed,  $k_j$  is jam density,  $v_m$  is optimal speed,  $k_m$  is optimal density, and  $n$  is an exponent.

of about 15 vehicles per kilometer or 25 vehicles per mile before a noticeable speed drop can be observed.

Inspired by Greenshields's pioneering work, many models were proposed subsequently to formulate speed-density relationships with various degrees of fitting quality. Table 4.1 provides an incomplete list of these early models.

The models in Table 4.1 share one thing in common—they are one-equation models, meaning that the models apply to the entire range of density. Hence, these models are called *single-regime models*. Figure 4.9 shows the performance of these single-regime models by plotting them on top of empirical observations, just to provide some visual feedback of how they approximate reality.

## 4.2 MULTIREGIME MODELS

It seems that none of these single-regime models are able to fit the empirical observations reasonably well over the entire density range. Some models are good in one density range, while others are superior in another range. The inability of single-regime models to perform well over the entire range of density prompted researchers to think about fitting the data in a piecewise manner using multiple equations. This gave rise to *multiregime models*, an incomplete list of which is given in Table 4.2. Among the list are the Edie model [16], the two-regime linear model, the modified Greenberg model, and the three-regime model.

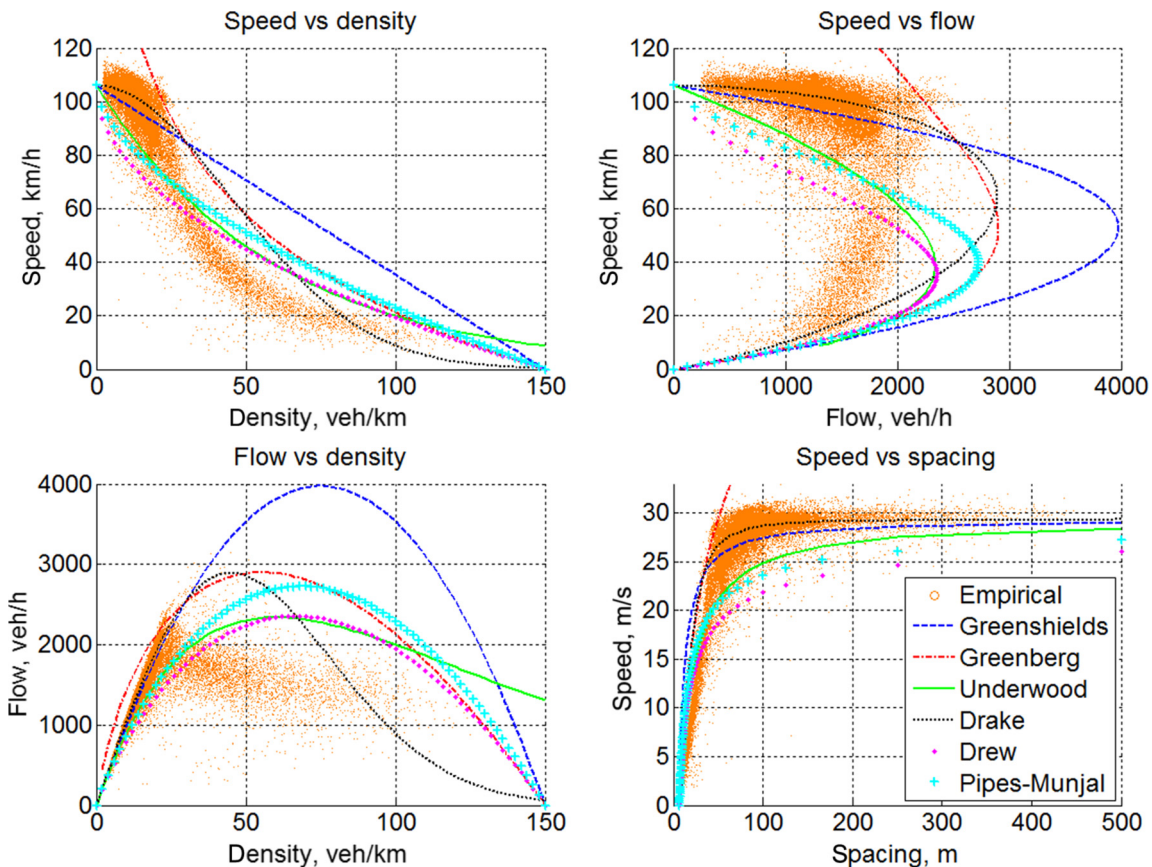


Figure 4.9 Comparison of single-regime models.

**Table 4.2** Multi-regime models

Regimes models	Free flow	Transitional	Congested
Edie model	$v = 108e^{-k/163.9}$ $k \leq 20$	- -	$v = 47\ln(162.5/k)$ $k > 20$
Two-regime model	$v = 108 - 0.515k$ $k \leq 30$	- -	$50 - 0.33k$ $k > 30$
Modified Greenberg model	$v = 103$ $k \leq 20$	- -	$v = 52\ln(150/k)$ $k > 20$
Three-regime model	$v = 108 - 0.5k$ $k \leq 20$	$v = 120 - 1.5k$ $20 < k \leq 65$	$v = 40 - 0.256k$ $k > 65$

May [17] presented a comparison of these multiregime models. Similar work illustrated in Figure 4.10 is found in Ref. [18].

### 4.3 THE STATE-OF-THE-ART MODELS

Early equilibrium models such as the Greenshields model [9], the Greenberg model [10], the Underwood model [11], the Drake model [12], the Drew model [13], and the Pipes-Munjal model [14, 15] are typically simple because they involve only two (the first four models) or three (the last two models) parameters. In addition, they are single-regime models whose derivatives of flow with respect to density ( $\frac{dq}{dk}$ ) exist at each point in the entire range of density. This makes these models mathematically appealing because  $\frac{dq}{dk}$  can be very useful later in dynamic macroscopic modeling such as in solving the LWR model (see Chapter 8). Moreover, these macroscopic models are closely related to a family of microscopic car-following models, and we shall revisit such a connection in Section 14. Unfortunately, these models typically suffer from poor fitting quality, as can be seen in Figure 4.9. Multiregime models such as the Edie model [16], the two-regime linear model, the modified Greenberg model, and the three-regime model may come with a little improvement in fitting quality, but their piecewise formulation makes them less attractive.

Further research emphasizes single-regime models, which are apparently coupled with the development of microscopic car-following models. Details of these car-following models and their associated equilibrium models will be discussed in Part III. Highlighted below are a set of more recent equilibrium models.

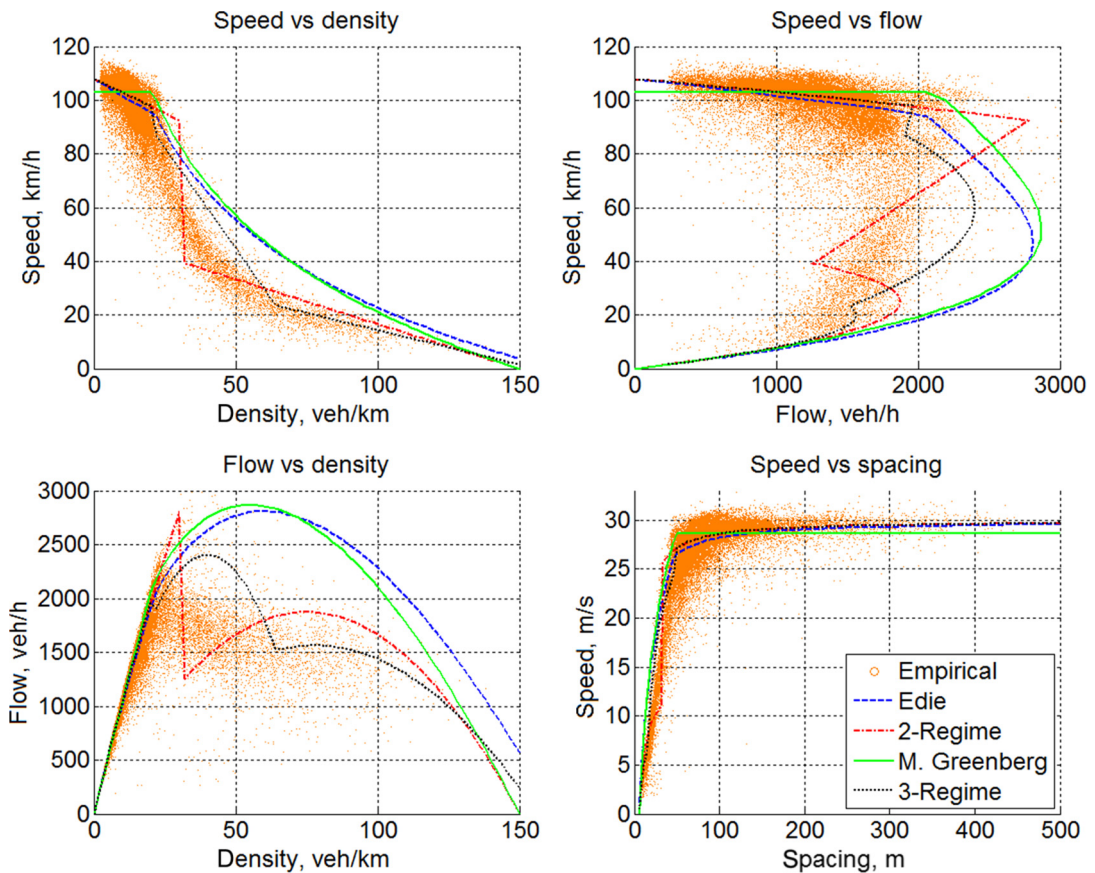


Figure 4.10 Comparison of multiregime models.

### Newell Nonlinear Model

The Newell nonlinear model [58] involves three parameters and takes the following form:

$$\nu = \nu_f \left( 1 - e^{-\frac{\lambda}{\nu_f} (\frac{1}{k} - \frac{1}{k_j})} \right),$$

where  $\nu_f$  is the free-flow speed,  $k_j$  is the jam density, and  $\lambda$  is the slope of the speed-spacing curve.

### Del Castillo and Benítez Model

Also involving three parameters, the model of del Castillo and Benítez [118, 131] takes the following form:

$$\nu = \nu_f \left( 1 - e^{1 - e^{\frac{|C_j|}{\nu_f} (\frac{k_j}{k} - 1)}} \right),$$

where  $\nu_f$  is the free-flow speed,  $k_j$  is the jam density, and  $C_j$  is the kinematic wave speed at the jam density.

### Del Castillo Negative Power Model

Continuing the above effort, del Castillo [120] proposed a new set of models recently, among which the negative power model is reproduced below:

$$\varphi = [(\nu_f \rho)^{-\omega} + (1 - \rho)^{-\omega}]^{-1/\omega},$$

where  $\rho = \frac{k}{k_j}$  and  $\varphi = \frac{q}{q_0}$ , where  $q_0$  is the reference flow, and  $\nu_f = -\frac{\nu_f}{C_j}$ . As such, this model involves five parameters: reference flow  $q_0$ , jam density  $k_j$ , free-flow speed  $\nu_f$ , kinematic wave speed at jam density  $C_j$ , and  $\omega$ .

Unlike other models in this subsection which result from the corresponding car-following models, the models of del Castillo [118, 120, 131] do not have their microscopic counterparts.

### Van Aerde Model

The Van Aerde model [62, 63] involves four parameters and takes the following form:

$$k = \frac{1}{c_1 + c_3 \nu + c_2 / (\nu_f - \nu)},$$

where  $c_1 = \frac{\nu_f}{k_j \nu_m^2} (2\nu_m - \nu_f)$ ,  $c_2 = \frac{\nu_f}{k_j \nu_m^2} (\nu_f - \nu_m)^2$ , and  $c_3 = \frac{1}{q_m} - \frac{\nu_f}{k_j \nu_m^2}$ . As such, the parameters of this model are the free-flow speed  $\nu_f$ , the optimal speed  $\nu_m$ , the capacity  $q_m$ , and the jam density  $k_j$ .

### ***Intelligent Driver Model***

The intelligent driver model [60, 61] involves four parameters and takes the following form:

$$k = \frac{1}{(s_0 + \nu T)[1 - (\frac{\nu}{\nu_f})^\delta]^{-1/2}}.$$

where parameters are free-flow speed  $\nu_f$ , jam distance  $s_0$ , safe time headway  $T$ , acceleration exponent  $\delta$ .

### ***Longitudinal Control Model***

The longitudinal control model [113] involves four parameters and takes the following form:

$$k = \frac{1}{(\gamma \nu^2 + \tau \nu + l)[1 - \ln(1 - \frac{\nu}{\nu_f})]},$$

where  $\nu_f$  is the free-flow speed,  $l$  is the nominal vehicle length (which is the reciprocal of the jam density,  $l = \frac{1}{k_j}$ ),  $\tau$  is the perception-reaction time, and  $\gamma$  is the aggressiveness.

To illustrate their features, the above models are fitted to empirical data. Although no effort is made to optimize the parameters, the following general principles apply when one is fitting the models: (1) fix the free-flow speed  $\nu_f$  of all the models to roughly the same value observed in the data, (2) fix the jam density  $k_j$  of all the models to roughly the same value observed in the data, and (3) fix the capacity to roughly the same value observed in the data by tweaking the remaining parameters. The resulting parameter values are listed in [Table 4.3](#) and the fitted models are illustrated in [Figure 4.11](#).

**Table 4.3** Model parameters

Models	Parameters
Newell model	$\nu_f = 106 \text{ km/h}; k_j = 167 \text{ vehicles/km}; \lambda = 1.25 \text{ 1/s}$
Del Castillo and Benítez model	$\nu_f = 106 \text{ km/h}; k_j = 167 \text{ vehicles/km}; C_j = 20 \text{ km/h}$
Negative power model	$\nu_f = 106 \text{ km/h}; k_j = 167 \text{ vehicles/km}; C_j = -16.56 \text{ km/h}; \omega = 50$
Van Aerde model	$\nu_f = 106 \text{ km/h}; k_j = 167 \text{ vehicles/km}; \nu_m = 20 \text{ km/h}; q_m = 2400 \text{ veh/h}$
Intelligent driver model	$\nu_f = 106 \text{ km/h}; s_0 = 6 \text{ m}; T = 1.25 \text{ s}; \delta = 15$
Longitudinal control model	$\nu_f = 106 \text{ km/h}; l = 6 \text{ m}; \tau = 1.3 \text{ s}; \gamma = -0.04 \text{ s}^2/\text{m}$

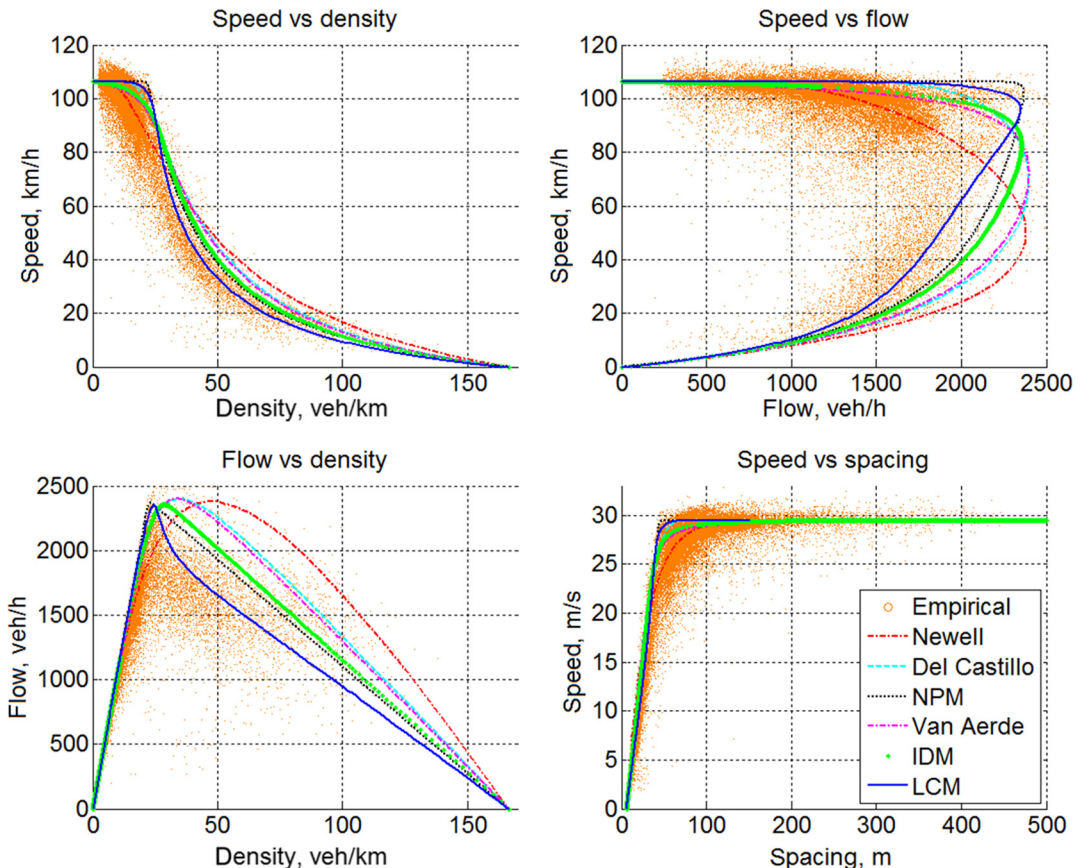


Figure 4.11 State-of-the-art models fitted to empirical data

Although many criteria have been proposed to evaluate fitting quality and a few algorithms have been developed to optimize the fitting process, the following reality check can be used as a visual inspection of the fitting quality:

1. **Free-flow speed** can be directly read off speed-density and speed-flow diagrams as the  $y$ -intercept. It is also the slope of the tangent to the flow-density curve that passes through the origin. It is typically not an issue to meet this criterion since one can easily estimate a value from empirical data and fix the model parameter free-flow speed  $v_f$  directly at this value.
2. **Jam density** can also be estimated from empirical data by following the trend of the tail of the scatter plot in the speed-density or flow-density diagram. Consequently, this value can be used to set the model parameter jam density  $k_j$  or the nominal vehicle length  $l = \frac{1}{k_j}$ . With the above two ends fixed, it is a good test of fitting quality to examine the capacity condition, which constitutes the third point of interest between the above two points.
3. The **capacity condition** includes the following checkpoints:
  - a. *The location of the capacity* ( $q_m$ ,  $k_m$ ,  $v_m$ ), where capacity  $q_m$  is the peak of the flow-density or speed-flow curve, and  $k_m$  and  $v_m$  are the optimal density and the optimal speed at capacity, respectively.
  - b. *The shape of the curve around the capacity* may exhibit the following types:
    - Skewed parabola: typically observed in outer-lane traffic
    - Triangular: typically observed in middle-lane traffic
    - Reverse-lambda shape: typically observed in inner-lane traffic

In Figure 4.11, the location of the capacity can be easily identified in speed-flow and flow-density diagrams as the tips of the curves. In addition, all three curve shapes can be found. Note that longitudinal control model can even be configured to exhibit the reverse-lambda shape in addition to the other two types.

## 4.4 CAN WE GO ANY FURTHER?

Though all relationships presented above take deterministic forms, the actual relationships are essentially quite random. For example, a speed-density relationship may predict that when the density  $k$  is 12 vehicles per kilometer or 20 vehicles per mile, the speed  $v$  will be 96 km/h or 60 miles per hour. However, in reality, the observed speed may vary over a certain range, forming a distribution (see Figure 4.12). The significance of these models lies in their ability to predict a value that makes statistical sense. For example, if one observes traffic for sufficiently long and collects enough speed samples,

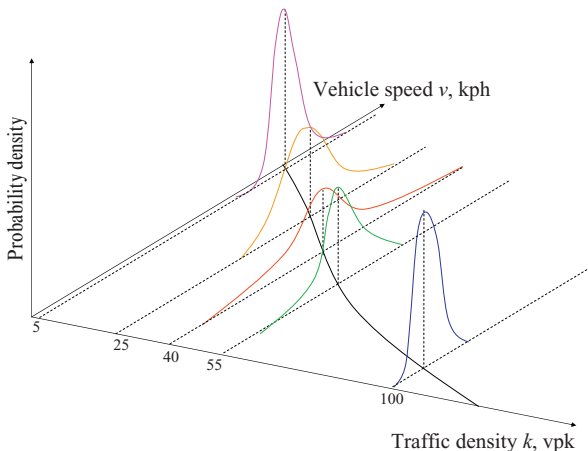


**Figure 4.12** Three-dimensional representation of the speed-density relationship.

the likelihood of having a speed in the neighborhood of 96 km/h or 60 miles per hour is very high. Figures 4.9 and 4.10 illustrate the scattering effect of empirical observations and how deterministic models fail to capture such an effect.

Therefore, a step forward to advance the modeling of the speed-density relationship and hence its associated fundamental diagram is to consider the scattering effect by representing speed as a distribution at each density level (see Figure 4.12). Empirical observations seem to support such a proposition. For example, in Figure 4.13 the observed mean and standard deviation of the speed-density relationship are plotted in a single figure. Hence, the deterministic speed-density relationship in the form

$$v = f(k)$$

may be replaced by the following one in generic form:

$$v = f(k, \omega(k)),$$

where  $\omega$  is a distribution parameter dependent (at least) on density  $k$ . In this model, since speed will be a distribution at each density level, the model is essentially a stochastic one. Readers are referred to [18–20] for attempts to obtain stochastic speed-density relationships.

The above pairwise relationships (i.e., equilibrium models) will become handy in the next chapter when we are setting up equations for macroscopic modeling and later for solving the LWR model.

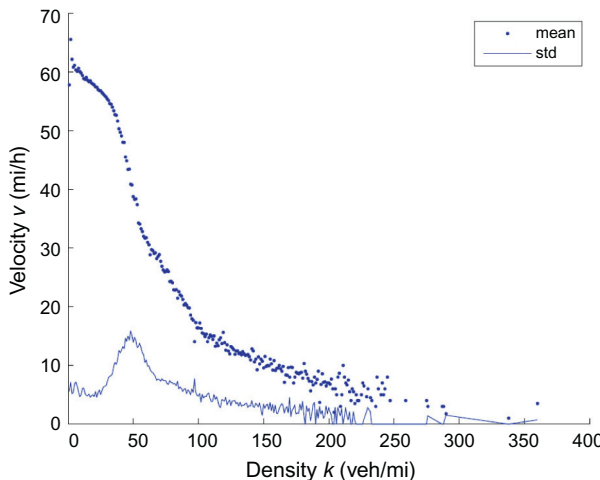
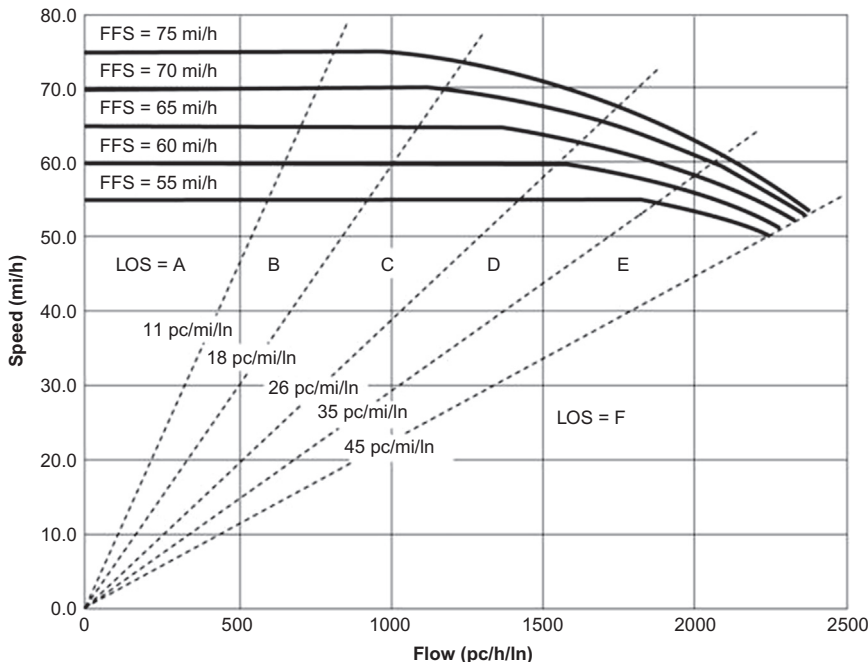


**Figure 4.13** Mean and variance of the speed-density relationship.

## PROBLEMS

1. From the linear speed-density relationship  $v = v_f (1 - k/k_j)$ , derive flow-density and speed-flow relationships. With these relationships, find the capacity  $q_m$  and the optimal speed  $v_m$  and density  $k_m$  when the capacity is reached.
2. Study of traffic flow characteristics on a segment of Massachusetts Turnpike (Interstate 90) shows that the following flow-density relationship holds:  $q = 65k - 0.36k^2$  pc/h/ln.
  - a. Find the optimal speed, optimal density, and the capacity of this highway segment.
  - b. Comment on how realistic the capacity is.
  - c. In addition, find the speed when the highway is at half of its capacity.
  - d. Comment on whether the above result makes sense.
3. The figure below is the speed-flow relationship used in the HCM to determine the LOS on a basic freeway segment and multilane highways. Use the curve labeled “FFS = 70 mi/h” to do the following:
  - a. Find the free-flow speed  $v_f$  indicated by this curve.
  - b. Find the capacity  $q_m$  indicated by this curve.
  - c. Find the optimal speed  $v_m$  indicated by this curve.
  - d. Estimate the optimal density  $k_m$  with use of the identity.
  - e. What LOS does this  $k_m$  correspond to?



- f. If the Greenshields model applies, calculate the jam density  $k_j$ , and further optimal density  $k_m$ .
- g. What LOS does this  $k_m$  corresponds to?
- h. Comment on how the Greenshields model approximates the HCM curve.
4. Derive the capacity  $q_m$  implied by the Greenberg model and find its associated optimal density  $k_m$ .
5. Derive the capacity  $q_m$  implied by the Underwood model and find its associated optimal speed  $v_m$ .
6. An engineering student estimated a free-flow speed of 60 miles per hour and a capacity of 3600 vehicles per hour on a section of highway. For a given period, a space mean speed of 45 miles per hour was estimated. If the Underwood model applies, what would you estimate the flow rate of this period to be?
7. On a section of Interstate 91 near the University of Massachusetts Amherst, studies show that the speed- density relationship is  $v = v_f[1 - ((k/k_j)^{2.5})]$ . Assume a capacity of 4600 vehicles per hour and that the

jam density is 200 vehicles per mile. Find the free-flow speed and the optimal speed at capacity.

8. Payne [21] proposed an early empirical speed-density relationship and used this relationship in his macroscopic traffic simulation model FREFLO:

$$\nu = \min\{88.5, (172 - 3.72k + 0.0346k^2 - 0.00119k^3)\},$$

where  $\nu$  is in kilometers per hour and  $k$  is in vehicles per kilometer.

- a. Plot the speed-density relationship graphically (you may draw it manually, do it in Excel, or use a computer program such as MATLAB). Use the plot to do the following:
- b. Identify the free-flow speed  $\nu_f$ .
- c. Identify the valid range of the density  $k$  in this model—that is, the range of  $k$  that yields nonnegative speed. Label the jam density  $k_j$  as the upper bound of this range.
- d. Identify the capacity condition—that is, capacity  $q_m$ , optimal speed  $\nu_m$ , and optimal density  $k_m$ .